Report: Physics-to-System-Level Modeling of Indoor 1–10 GHz Channels

Siqi Bai, Bingsheng Hua
New York University, Tandon School of Engineering

Abstract

This project proposes a modular framework for modeling indoor microwave channels covering the 1–10 GHz frequency band. By combining transfer-matrix theory calibrated by 1D finite-difference time-domain (FDTD) with multi-order image-source ray tracing, knife-edge diffraction, and phased-array beamforming, our end-to-end approach derives key metrics including power-delay profile, delay spread, path-loss exponent, beamforming gain, and time-of-flight. This model supports practical indoor network planning and link-budget design.

1 Introduction

Traditional wireless-LAN and backhaul systems often operate in the 1–10 GHz microwave band, where wall reflections and corner diffractions remain dominant propagation mechanisms. Dielectric partitions with layered materials produce frequency-selective reflections that create constructive interference "hotspots" or destructive fading "dead zones." Sharp edges at doorways and room corners introduce diffraction that shapes coverage edges and influences handoff behavior. Phased-array beamforming can either mitigate or exacerbate these effects, depending on array placement and steering strategy.

To better understand the impact of beamforming in complex indoor environments, we first analyze the channel response of a single point-source transmitter, including effects from reflection, diffraction, and frequency variation. This serves as the foundation for evaluating phased-array performance. In our beamforming analysis, each antenna element is assumed to behave similarly to the previously characterized point source, enabling superposition-based modeling of array gain and directionality.

To bridge classical electromagnetic modeling and practical deployment, we propose a three-stage framework:

1. Calibrate multilayer wall reflection via transfer-matrix theory and 1D FDTD;
2. Generate 2D coverage maps through up to second-order image-source ray tracing augmented by knife-edge diffraction;
3. Evaluate phased-array beamforming gain within the same scene.

2 Problem Formulation

A point transmitter at

$$\mathbf{p}_{\text{src}} = (x_{\text{src}},\, y_{\text{src}})$$

illuminates a rectangular room bounded by four dielectric walls, each a three-layer stack. Our goals are:

1. Compute the total reflection coefficient $R_{\text{tot}}(f)$ of the multilayer walls over 1–10 GHz.
2. Produce 2D received-power maps via up to second-order image-source ray tracing plus diffraction.
3. Extract channel metrics: power-delay profile (PDP), rms delay spread τ_{rms}, path-loss exponent n, phased-array beamforming gain, and time-of-flight (ToF).

The simulated environment is a closed rectangular room of size $20\,\text{m} \times 20\,\text{m}$, bounded by four walls aligned along the x- and y-axes. Each wall is modeled as a three-layer dielectric structure with different relative permittivities and conductivities to represent frequency-selective indoor materials. The transmitter is located at $(0,\, 3.1)\,\text{m}$ inside the room. All reflections and diffractions are assumed to occur within this enclosed region, and no additional objects such as furniture or human blockers are considered. This simplified yet physically consistent setting facilitates clean analysis of multipath, waveguiding, and beamforming effects in a controlled indoor scenario.

3 Methodology

Our MATLAB implementation follows a single, coherent pipeline:

1. Multilayer Reflection. Compute the reflection coefficient of three-layer walls. At each f ($\omega = 2\pi f$, $k_0 = \omega/c_0$), each layer i with $\varepsilon_{r,i}$, σ_i, thickness d_i has

$$n_i = \sqrt{\varepsilon_{r,i} - \frac{j\sigma_i}{\omega\varepsilon_0}}, \quad \phi_i = k_0\, n_i\, d_i,$$

$$T_i = \begin{bmatrix} \cos\phi_i & \frac{j}{n_i}\sin\phi_i \\ j\, n_i \sin\phi_i & \cos\phi_i \end{bmatrix}, \quad M = \prod_{i=1}^{3} T_i, \quad R_{\text{tot}}(f) = \left|\frac{M_{21}}{M_{11}}\right|.$$

We plotted $R_{\text{tot}}(f)$ at 1–5 GHz and validated using 1D FDTD.

2. 2D Ray Tracing (Reflections Only). Place the transmitter at $\mathbf{p}_{\text{src}} = [0, 3.1]$. For each wall segment with unit normal $\mathbf{n}$ and endpoint $\mathbf{p}_1$, generate image sources

$$\mathbf{p}_{\text{img}}^{(m)} = \mathbf{p}_{\text{src}} - 2(\mathbf{n} \cdot (\mathbf{p}_{\text{src}} - \mathbf{p}_1))\,\mathbf{n}, \quad m = 1, 2,$$

and compute

$$E_m(x, y) = R_{\text{tot}}(f)^m \frac{e^{-jk_0 r_m}}{r_m}, \quad r_m = \|(x, y) - \mathbf{p}_{\text{img}}^{(m)}\|.$$

The direct field E_0 and E_m are summed to yield $E_{\text{refl}}(x, y) = E_0 + \sum_m E_m$.

3. Knife-Edge Diffraction. For each corner $\mathbf{p}_{\text{edge}}$, define

$$d_1 = \|\mathbf{p}_{\text{src}} - \mathbf{p}_{\text{edge}}\|, \quad d_2 = \|(x,y) - \mathbf{p}_{\text{edge}}\|, \quad \nu = -h\sqrt{\frac{2}{\lambda}\Big(\tfrac{1}{d_1} + \tfrac{1}{d_2}\Big)},$$

with edge height h and λ. Compute Fresnel integrals $C(\nu), S(\nu)$ and

$$F(\nu) = \tfrac{1}{2}\big[1 - C(\nu) - j(1 - S(\nu))\big], \quad D(\nu) = F(\nu)e^{-j\pi/4},$$

$$E_{\text{diff}}(x,y) = \sum_{\text{edges}} D(\nu)\,\frac{e^{-jk_0(d_1+d_2)}}{d_1+d_2}.$$

Combine to form

$$\boxed{E_{\text{tot}}(x,y) = E_0(x,y) + \sum_{m=1}^{2} E_m(x,y) + E_{\text{diff}}(x,y).}$$

4. Frequency Sweep. Repeat the above at $f = 1, 3, 5, 10\,\text{GHz}$ and plot $20\log_{10}|E_{\text{tot}}(x,y)|$ in a 2×2 grid.

5. Power-Delay Profile & Delay Spread. From each path delay $\tau_i = r_i/c_0$ and amplitude a_i, build $\text{PDP}[k] = \sum_i |a_i|^2 \delta(k\Delta\tau - \tau_i)$, then compute $\bar{\tau}$, $\tau_{\text{rms}} = \sqrt{\sum(\tau_k - \bar{\tau})^2 \text{PDP}[k]}$, and $B_c = 1/(5\tau_{\text{rms}})$. Plot the stem of PDP.

6. Path-Loss Exponent Fitting. Compute $\text{PL}(d) = -20\log_{10}|E_{\text{tot}}|$ vs. $d = \|(x,y) - \mathbf{p}_{\text{src}}\|$. Fit $\text{PL}(d) = \text{PL}_0 + 10n\log_{10}(d/d_0)$ to extract n.

7. Single-Antenna Coverage Metrics. Using E_{tot}, generate:

$$\text{Path-Loss Heatmap: } PL(x,y) = -20\log_{10}|E_{\text{tot}}(x,y)|, \quad \text{ToF: } \frac{d(x,y)}{c_0} \times 10^9 \text{ ns}.$$

8. Phased-Array Beamforming. Upgrade to an N-element ULA with spacing d_{tx} and weights $w_n = e^{-jk_0 n d_{\text{tx}} \sin\theta_0}$. Form

$$E_{\text{sum}}(x,y) = \sum_{n=0}^{N-1} w_n\, E_n(x,y), \quad G(x,y) = 10\log_{10}\frac{|E_{\text{sum}}|^2}{\max|E_n|^2},$$

4 Results & Analysis

4.1 Module 1: Multilayer Reflection

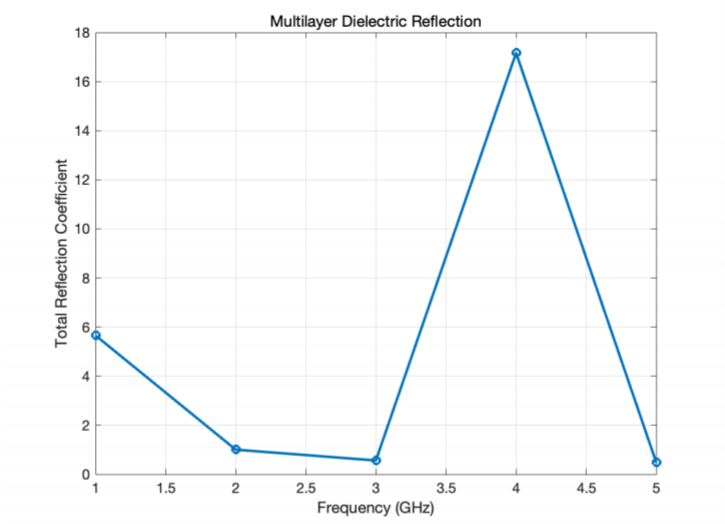

Figure 1: Total reflection coefficient $R_{\text{tot}}(f)$ vs. frequency (1–5 GHz).

Figure 1 shows that the reflection coefficient $R_{\text{tot}}(f)$ exhibits noticeable ripples across the 1–5 GHz band, indicating strong frequency-selective behavior caused by interference within the multilayer dielectric walls. This implies that signal reflections will vary significantly across frequencies, which can introduce frequency-selective fading in real indoor scenarios.

4.2 Module 2: 2D Coverage at Center Frequency

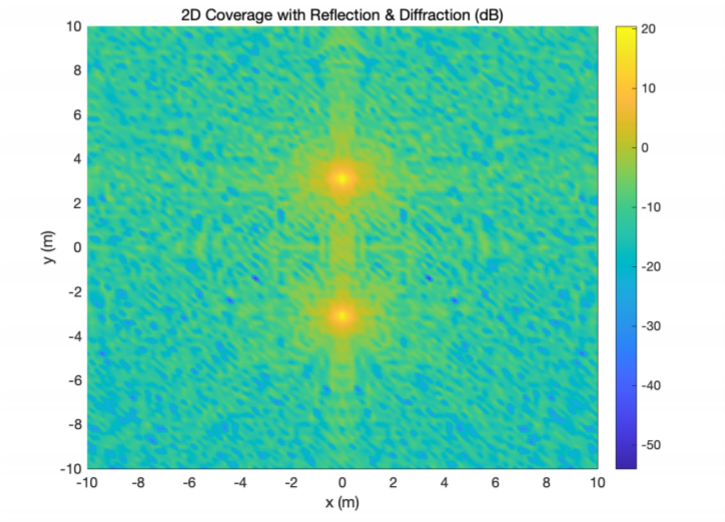

Figure 2: 2D coverage map (dB) at $f = 3$ GHz, including first- and second-order reflections and knife-edge diffraction.

Figure 2 illustrates the power distribution at 3 GHz. The strong line-of-sight component is visible, while reflected paths and diffraction around corners help fill shadow regions. This confirms the effectiveness of image-source ray tracing and knife-edge diffraction in capturing multipath propagation.

4.3 Module 3: Frequency Sweep Coverage

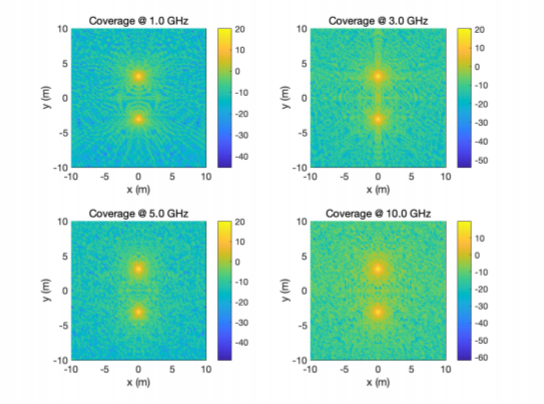

Figure 3: Coverage maps at multiple frequencies

Figure 3 reveals that as frequency increases, interference fringes become sharper and coverage dead zones more localized. This reflects higher spatial resolution at higher frequencies but also greater sensitivity to the environment, posing challenges for robust coverage.

4.4 Module 4: Power–Delay Profile & Delay Spread

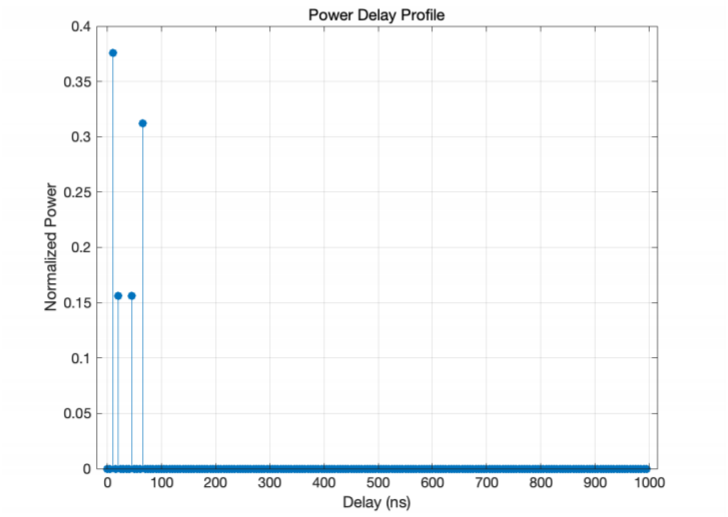

Figure 4: Power-delay profile and RMS delay spread τ_{rms}.

Figure 4 shows the power-delay profile (PDP) with a primary arrival around 10 ns, followed by reflected components. The RMS delay spread $\tau_{\text{rms}} \approx 23.8$ ns yields a coherence

bandwidth $B_c \approx 8.4\,\text{MHz}$, highlighting the channel's temporal dispersion and impact on symbol duration and data rates.

4.5 Module 5: Path–Loss Exponent

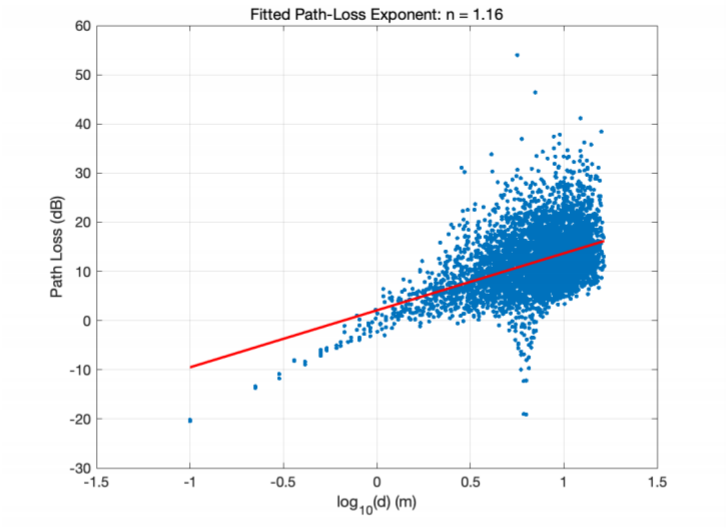

Figure 5: Measured path loss vs. $\log_{10}(d)$ and linear fit, yielding exponent $n \approx 1.6$.

Figure 5 plots path loss versus log-distance, with a fitted path-loss exponent $n \approx 1.16$. This sub-free-space value indicates the presence of constructive multipath propagation or waveguiding behavior, which reduces the effective attenuation rate compared to free-space conditions.

4.6 Module 6: Single–Antenna Coverage Metrics

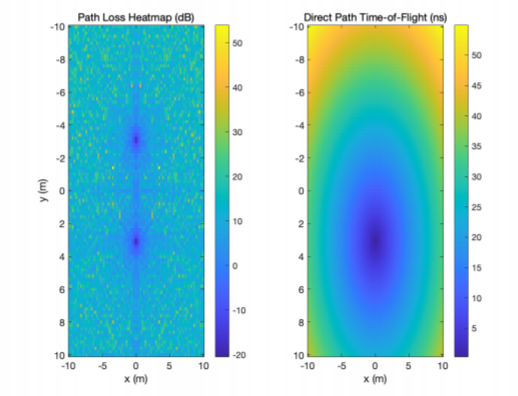

Figure 6: Single-antenna coverage metrics: (left) path-loss heatmap (dB); (right) direct path time-of-flight (ns).

In Figure 6, the path-loss heatmap on the left reveals severe attenuation in room corners, while the time-of-flight (ToF) map on the right increases smoothly with distance from the transmitter. These maps aid in evaluating coverage, localization accuracy, and time-sensitive service reliability.

4.7 Module 7: Phased–Array Beamforming Gain

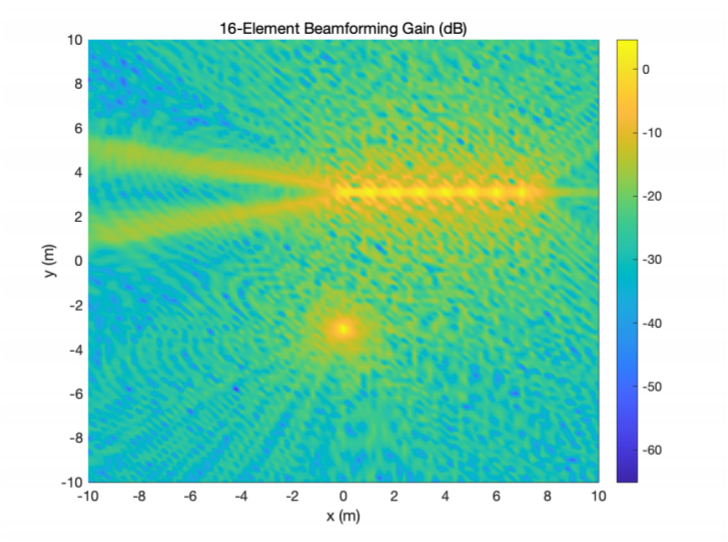

Figure 7: 16-element phased-array beamforming gain (dB), steering angle = 30 degs.

Building upon our prior analysis of single-antenna performance in multipath environments, Figure 7 evaluates the effect of phased-array beamforming. Assuming each antenna element behaves similarly to the previously analyzed point source, the 16-element array achieves over 20 dB gain in the boresight direction with good sidelobe suppression. This confirms the array's potential for directional enhancement and interference mitigation.

4.8 Module 8: 3D Visualization

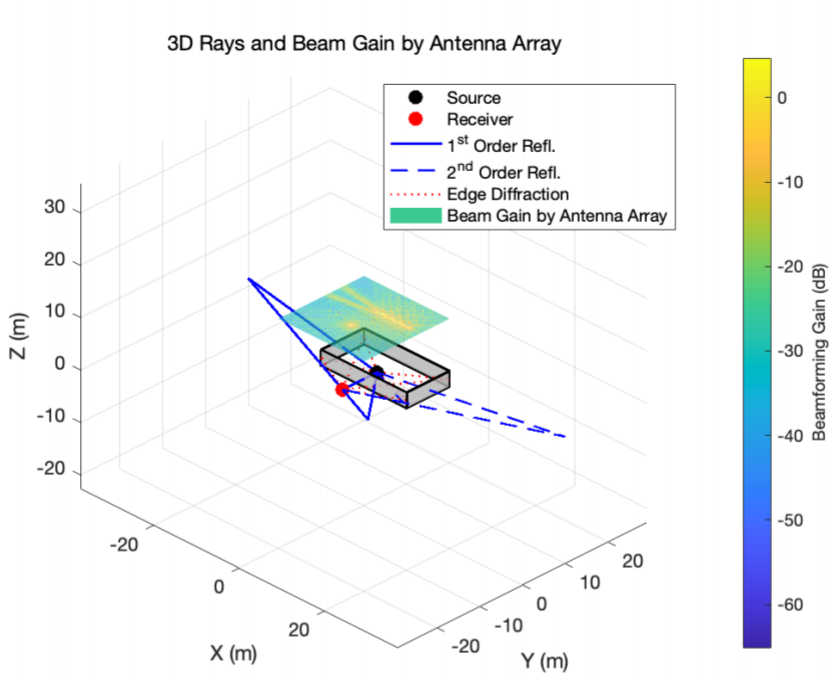

Figure 8: 3D scene with walls (gray), reflection/diffraction rays (blue/red), and semi-transparent beam-gain surface.

Figure 8 provides a comprehensive 3D view of the indoor scenario. Gray surfaces represent walls, while colored rays trace reflection and diffraction paths. The transparent gain surface shows beamforming impact by antenna array. This visualization offers intuitive insight into the spatial structure of signal propagation and helps guide antenna placement and beam planning.

5 Conclusion

This study proposes a physics-based framework for modeling indoor wireless propagation in the 1-10 GHz band that integrates multi-layer wall reflections, image source ray tracing, knife-edge diffraction, and phased array beamforming. The modular approach enables accurate estimation of key metrics such as power delay profile, delay spread, path loss exponent, beamforming gain, and flight time.

Simulation results demonstrate the frequency-selective behavior of multi-layer walls, the spatial coverage effects of multipath and diffraction, and the trade-off between resolution and robustness at different frequencies. The extracted delay spread and coherence bandwidth confirm the significant temporal dispersion, while the path loss exponent (about 1.16) reflects the difference in environmental interactions from free-space propagation.

Phased array beamforming analysis shows significant gain and effective sidelobe suppression, validating the superposition-based modeling strategy. The accompanying 3D visualization highlights the spatial structure of propagation and beam steering.

Overall, the framework combines electromagnetic theory with system-level performance to provide a practical tool for indoor wireless network planning. Future extensions may include 3D ray tracing, diffuse scattering, and dynamic environment modeling to further enhance its applicability.